**SUPPLEMENTARY INFORMATION**

# Spectral Tuning Mechanism of Primate Blue-Sensitive Visual Pigment Elucidated by FTIR Spectroscopy

Kota Katayama[1,2,a], Yuki Nonaka[1,a], Kei Tsutsui[3], Hiroo Imai[3], and Hideki Kandori[*,1,2]

[1]Department of Life Science and Applied Chemistry, Nagoya Institute of Technology, Showa-ku, Nagoya 466-8555, Japan

[2]OptoBioTechnology Research Center, Nagoya Institute of Technology, Showa-ku, Nagoya 466-855, Japan

[3]Primate Research Institute, Kyoto University, Inuyama 484-8506, Japan

[*]Corresponding authors: Department of Life Science and Applied Chemistry, Nagoya Institute of Technology, Showa-ku, Nagoya 466-8555, Japan. Phone and fax: 81-52-735-5207. E-mail: kandori@nitech.ac.jp.

[a]These authors contributed equally to this work.

**Table 1**

Table1: Frequency of HOOP bands (Table.1)

| | (-) $C_{11}$=$C_{12}$ HOOP | (+) $C_{11}$ HOOP | (+) $C_{12}$ HOOP | Δ ($C_{11}$-$C_{12}$ HOOP) | S[a] |
|---|---|---|---|---|---|
| MB | 961 | 928 | 865 | 63 | 0.00252 |
| MB Y265W | 963 | 924 | 865 | 59 | 0.00190 |
| MRh W265Y | 970 | 923 | 857 | 66 | 0.00299 |
| MRh | 966 | 917 | 857 | 60 | 0.00238 |
| MG | 973 | 907[b] | 848 | 59 | 0.00540 |
| MR | 973 | 906[c] | 847 | 59 | 0.00516 |

[a] Sum of the intensity of negative bands from $C_{11}$=$C_{12}$ HOOP

[b] Average of two positive bands (911$cm^{-1}$ and 903$cm^{-1}$)

[c] Average of two positive bands (909$cm^{-1}$ and 903$cm^{-1}$)

**Supplementary Figure legends**

***Figure S1.*** **Amino acid sequences of monkey blue, rhodopsin (bovine and monkey), monkey green, and monkey red.** (a) 26 amino acids within 5 Å from the retinal chromophore in the X-ray structure of bovine rhodopsin are shown. The amino acids are identical between bovine and monkey rhodopsins. The two key residues for monkey blue, Glu113 and Tyr265 are highlighted by red. The residue numbers are based on the bovine rhodopsin sequence. (b) Schematic representation of the 26 amino acid differences around 11-*cis*-retinal among each pigments.

***Figure S2***. **Light-induced difference FTIR and UV-visible absorption spectra of mutant proteins, and correlation between the retinal C=C stretching frequency and $\lambda_{max}$.** (a) Light-induced difference FTIR spectra of MB, MB-Y265W, MRh-W265Y, MRh, MG and MR in the 1800-800 $cm^{-1}$ region at 77 K. One division of the y-axis corresponds to 0.0013 absorbance units. (b) Expanded spectra from (a) in the 1630- 1450 $cm^{-1}$ region. One division of the y-axis corresponds to 0.0013 absorbance units. (c) UV-visible absorption spectra of MB ($\lambda_{max}$ = 417 nm), MB-Y265W ($\lambda_{max}$ = 434 nm), MRh-W265Y ($\lambda_{max}$ = 481 nm), MRh ($\lambda_{max}$ = 499 nm), MG ($\lambda_{max}$ = 530 nm) and MR ($\lambda_{max}$ = 563 nm). (d) Correlation of the unphotolyzed retinal C=C stretching frequencies of MB (1576 $cm^{-1}$), MB-Y265W (1566 $cm^{-1}$), MRh-W265Y (1564 $cm^{-1}$), MRh (1561 $cm^{-1}$), MG (1534 $cm^{-1}$) and MR (1526 $cm^{-1}$) from (b) with their absorption maxima from (c).

***Figure S3.*** **Structural changes from rhodopsin (green) to bathorhodopsin (red), and representation around retinal binding pocket.** (a) Structural changes from rhodopsin (green) to batho-intermediate state, bathorhodopsin (red) are viewed from extracellular side. The double bond at the position $C_{11}$ and $C_{12}$ ($C_{11}$=$C_{12}$) is highlighted about highly distortion. (b) Part of the retinal binding pocket are viewed from helix VI, where the curvature along the polyene chain of retinal is emphasised, and side chain of W265 is facing towards atoms of $C_{11}$ and $C_{12}$.

***Figure S4.*** **HOOP band correlation diagrams for dark and batho-intermediate state among each pigments with their absorption maxima, and summary of the HOOP band frequencies of the batho-intermediate state.** (a) Correlation of the $C_{11}$=$C_{12}$ HOOP band frequencies of different pigments in the dark state with their absorption maxima. (b) Correlation of the $C_{11}$ or $C_{12}$ HOOP band frequencies of different pigments in the batho-intermediate state with their absorption maxima. (c) Calculated area of $C_{11}$=$C_{12}$ HOOP band of different pigments in the dark state with their absorption maxima. (d) Summary of the HOOP band frequencies of different pigments in the batho-intermediate state.

***Figure S5.*** **Light-induced difference FTIR of MB, MB-Y265W, MRh-W265Y and MRh in the 3400-3200 cm$^{-1}$ region at 77 K.** One division of the y-axis corresponds to 0.0005 absorbance units.

***Figure S6.*** **Light-induced difference FTIR of MB (blue solid and dotted lines), MB-Y265W (light blue) and MB-E113D (magenta) in the 2730-2460 cm$^{-1}$ region at 77 K.** One division of the y-axis corresponds to 0.00016 absorbance units.

***Figure S7.*** **Light-induced difference FTIR of MB, MB-Y265W, MRh-W265Y, MRh, MG and MR in the 3600-3380 cm$^{-1}$ region at 77 K.** One division of the y-axis corresponds to 0.0005 absorbance units.

***Figure S8.*** **Light-induced difference FTIR of MB, MRh, MG and MR in the 2150-1930 cm$^{-1}$ region at 77 K.** One division of the y-axis corresponds to 0.00004 absorbance units.

# Figure S1

(a)

| | 113 | | | | | | | | | | | 125 | 164 | 181 | | | | | | | | | 191 |
|---|---|---|---|---|---|---|---|---|---|---|---|---|---|---|---|---|---|---|---|---|---|---|---|
| monkey blue (417nm) : | E | G | . | . | G | T | . | . | G | L | . | . | G | G | E | . | . | . | . | S | C | G | P | . | W |
| rhodopsin (499nm) : | E | G | . | . | A | T | . | . | G | E | . | . | L | A | E | . | . | . | . | S | C | G | I | . | Y |
| monkey green (530nm) : | E | G | . | . | V | S | . | . | G | I | . | . | L | A | H | . | . | . | . | S | C | G | P | . | V |
| monkey red (563nm) : | E | G | . | . | V | S | . | . | G | I | . | . | L | S | H | . | . | . | . | S | C | G | P | . | V |
| | Helix III | | | | | | | | | | | | | Helix IV | E-II loop | | | | | | | | |

| | 207 | | | 212 | 261 | | | 265 | | 269 | 292 | | | 296 |
|---|---|---|---|---|---|---|---|---|---|---|---|---|---|---|
| monkey blue (417nm) : | L | F | . | . C | F | F | . | . | . | Y | . | . Y | A | A | F | . S | K |
| rhodopsin (499nm) : | M | F | . | . H | F | F | . | . | . | W | . | . Y | A | A | F | . A | K |
| monkey green (530nm) : | L | M | . | . C | C | F | . | . | . | W | . | . Y | A | A | Y | . A | K |
| monkey red (563nm) : | L | M | . | . C | C | Y | . | . | . | W | . | . Y | T | A | Y | . A | K |
| | Helix V | | | | | Helix VI | | | | | | | | Helix VII | | | |

(b)

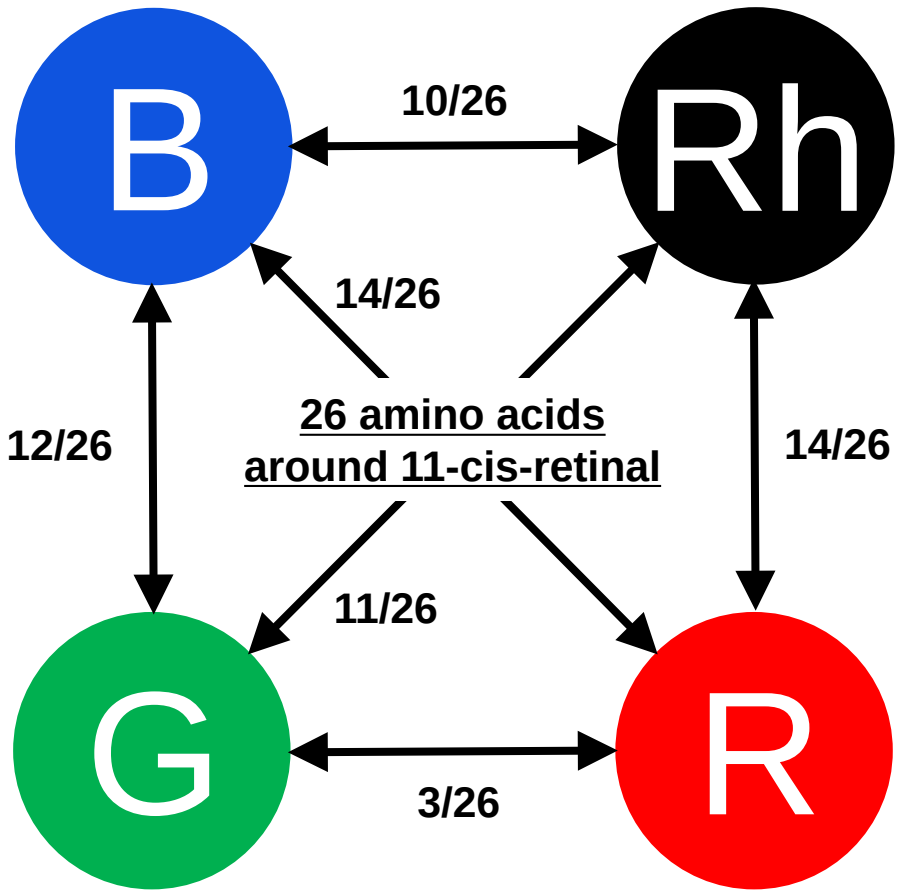

# Figure S2

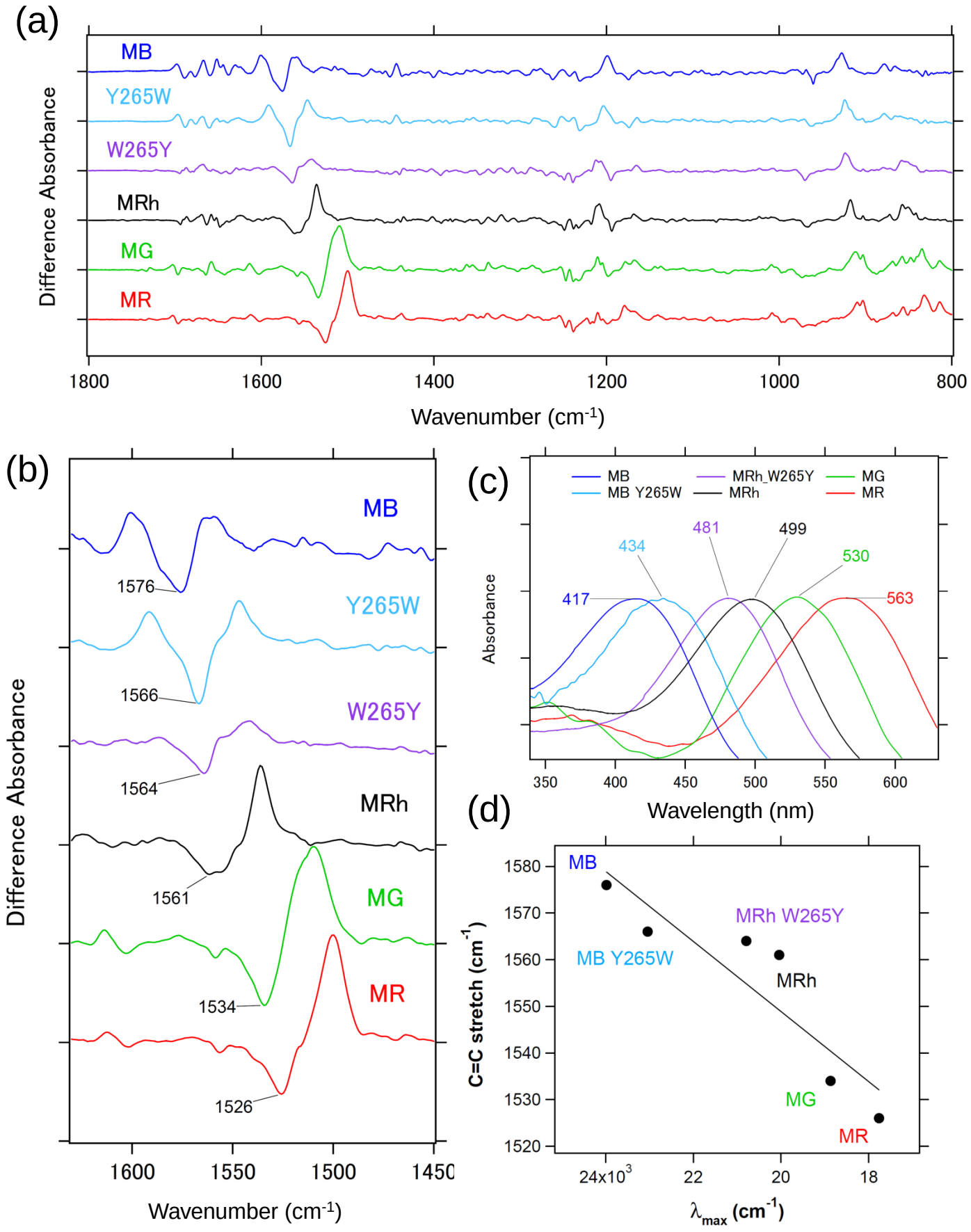
(a)
MB
Y265W
W265Y
MRh
MG
MR
Difference Absorbance
1800
1600
1400
1200
1000
800
Wavenumber (cm-1)
(b)
MB
1576
Y265W
1566
W265Y
1564
MRh
1561
MG
1534
MR
1526
Difference Absorbance
1600
1550
1500
1450
Wavenumber (cm-1)
(c)
MB
MB Y265W
MRh_W265Y
MRh
MG
MR
434
481
499
530
417
563
Absorbance
350
400
450
500
550
600
Wavelength (nm)
(d)
MB
MRh W265Y
MB Y265W
MRh
MG
MR
C=C stretch (cm-1)
1580
1570
1560
1550
1540
1530
1520
24x10^3
22
20
18
λmax (cm-1)

Figure S3

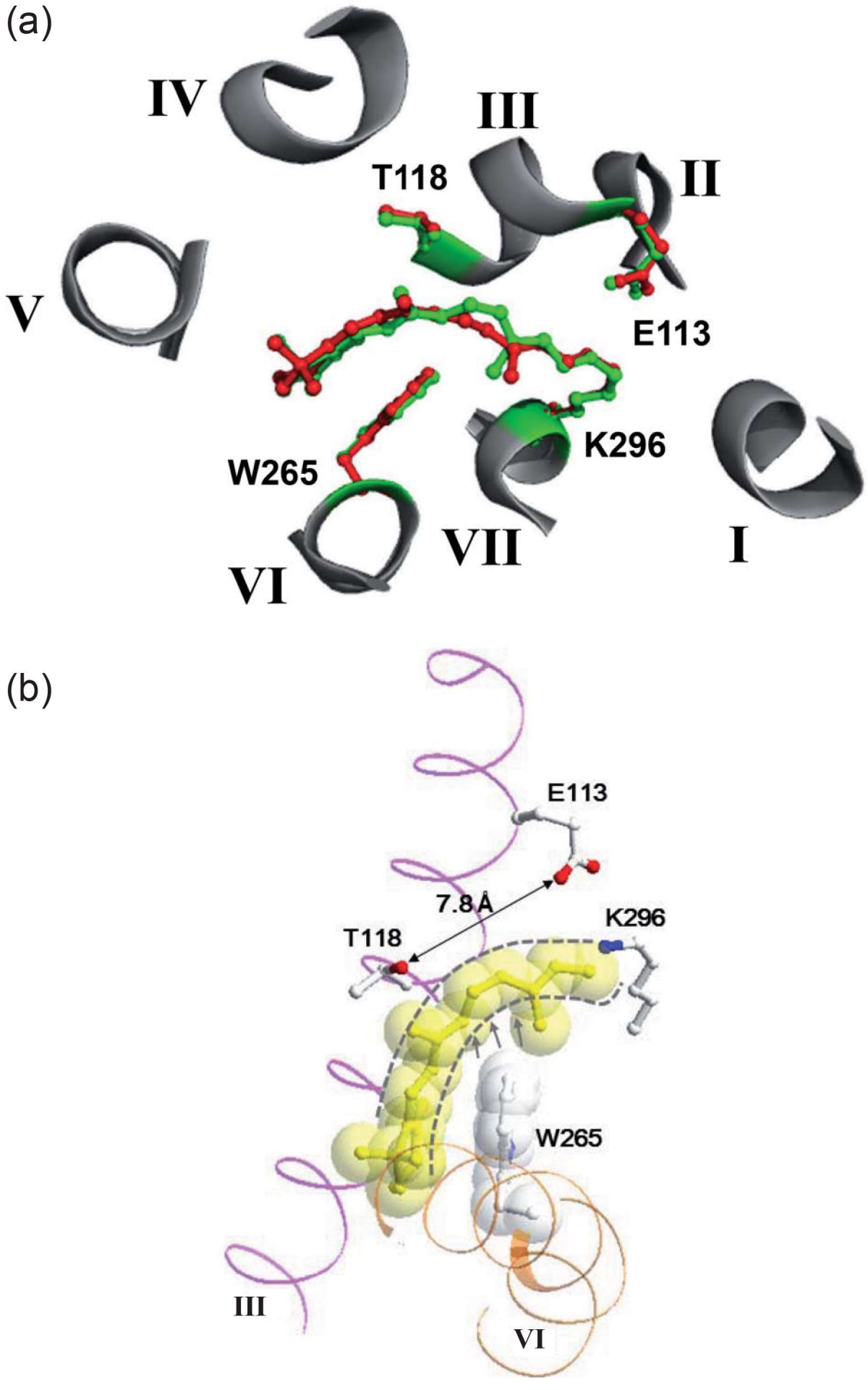
(a)
IV
III
T118
II
V
E113
K296
W265
VII
I
VI
(b)
E113
7.8 Å
K296
T118
W265
III
VI

Figure S4

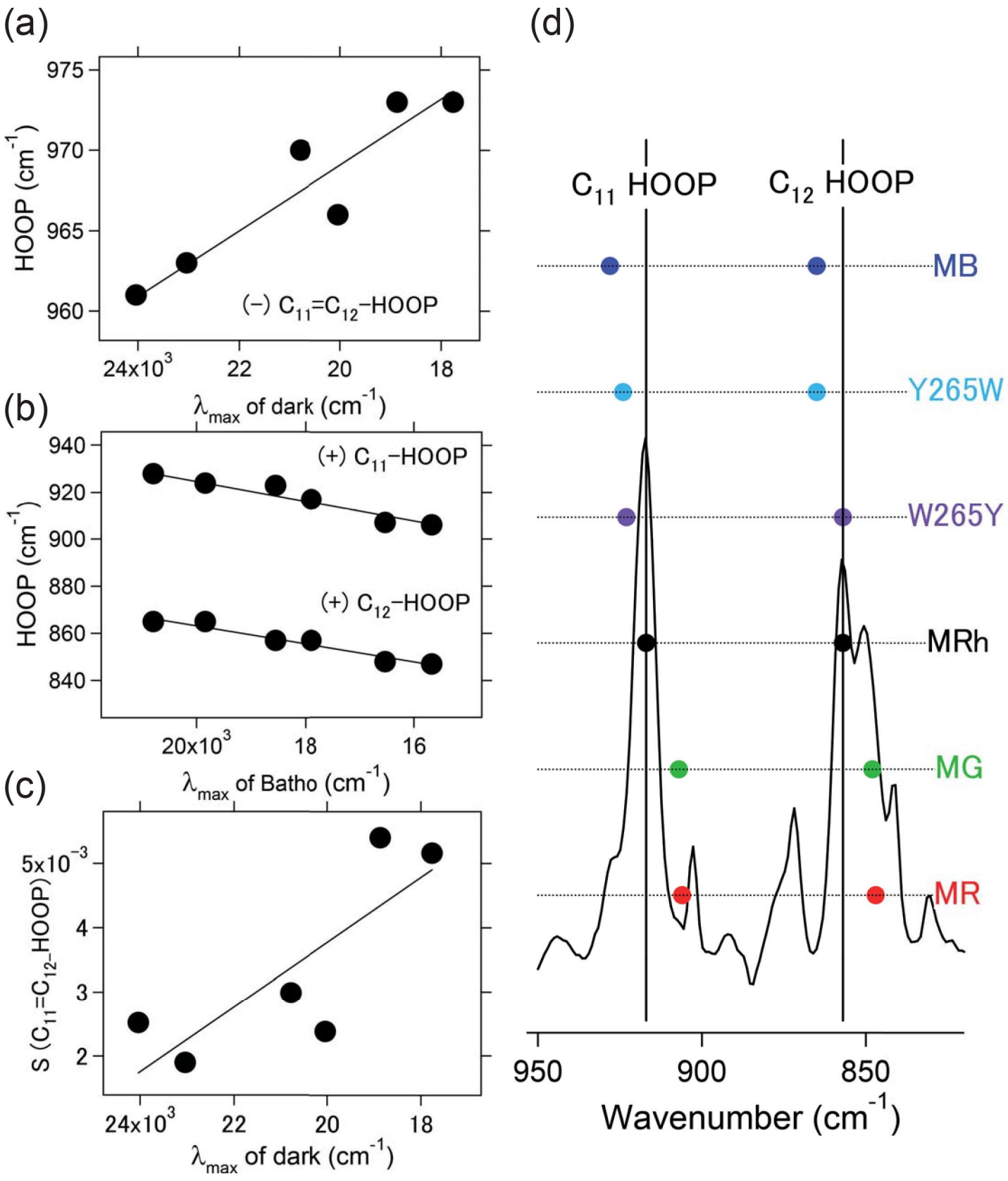
(a)
975
970
965
960
HOOP (cm-1)
(–) C11=C12–HOOP
24x10^3
22
20
18
λmax of dark (cm-1)
(b)
940
920
900
880
860
840
HOOP (cm-1)
(+) C11–HOOP
(+) C12–HOOP
20x10^3
18
16
λmax of Batho (cm-1)
(c)
5x10-3
4
3
2
S (C11=C12-HOOP)
24x10^3
22
20
18
λmax of dark (cm-1)
(d)
C11 HOOP
C12 HOOP
MB
Y265W
W265Y
MRh
MG
MR
950
900
850
Wavenumber (cm-1)

Figure S5

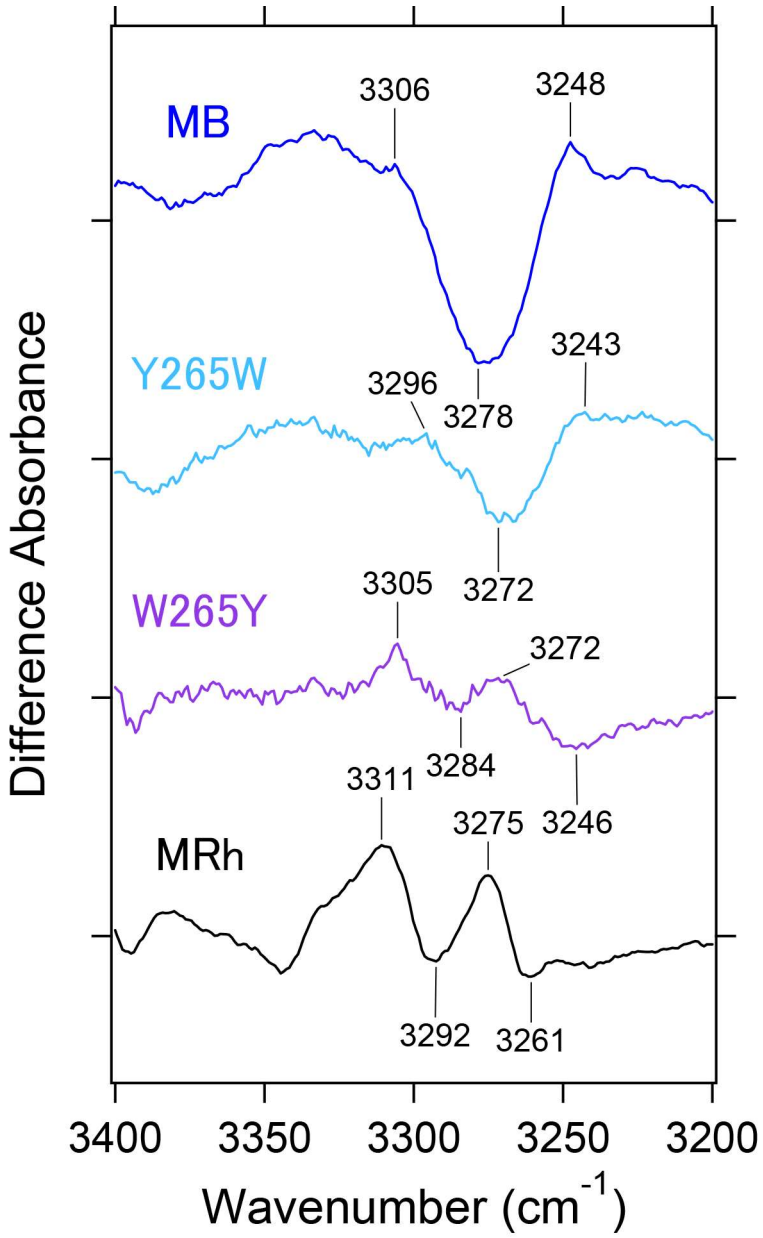
MB
3306
3248
Y265W
3296
3278
3243
W265Y
3305
3272
3284
3272
3246
MRh
3311
3275
3292
3261
Difference Absorbance
3400
3350
3300
3250
3200
Wavenumber (cm-1)

Figure S6

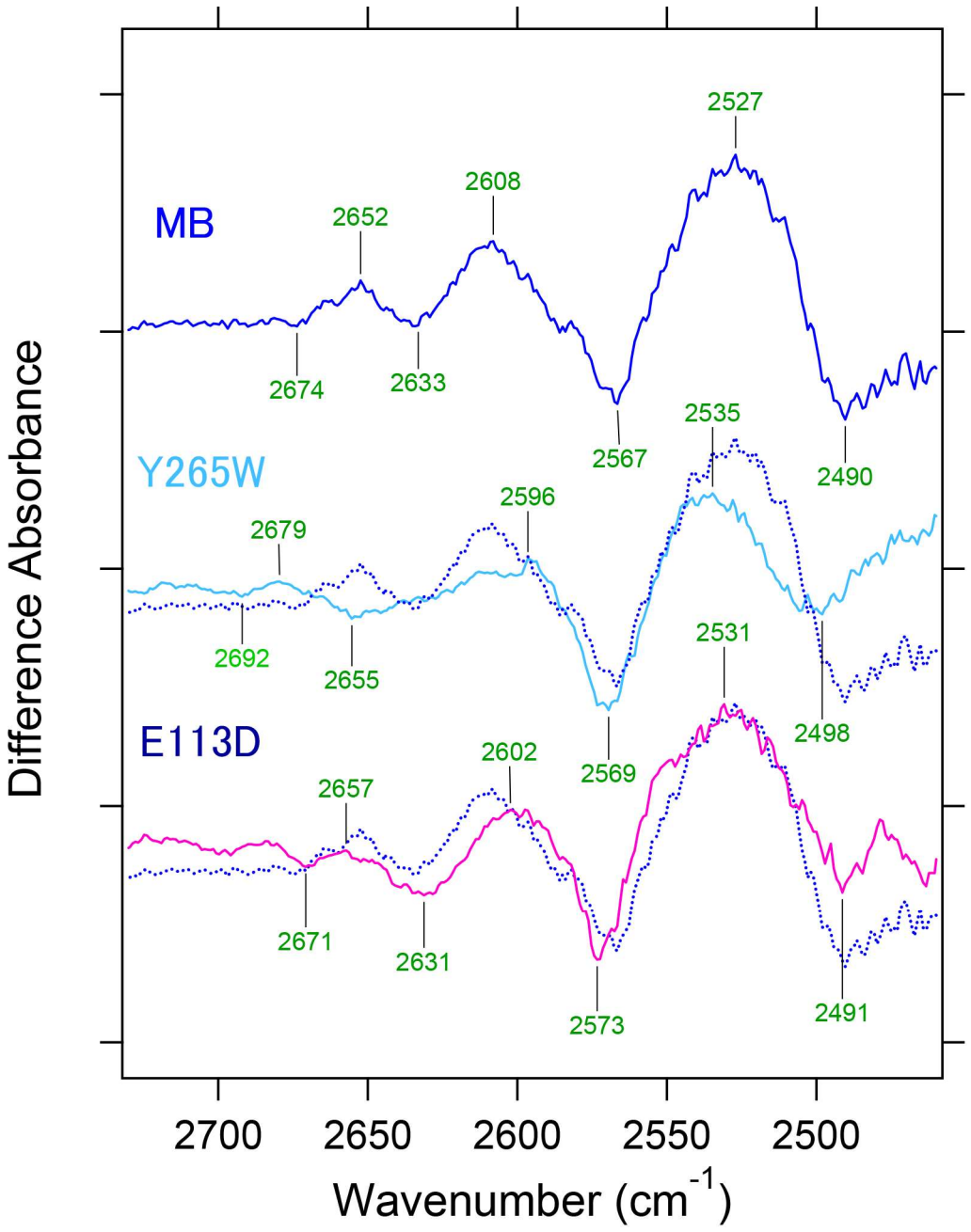
MB
2527
2608
2652
2674
2633
2567
2490
Y265W
2535
2596
2679
2692
2655
2531
2498
2569
E113D
2602
2657
2671
2631
2573
2491
Difference Absorbance
2700
2650
2600
2550
2500
Wavenumber (cm-1)

Figure S7

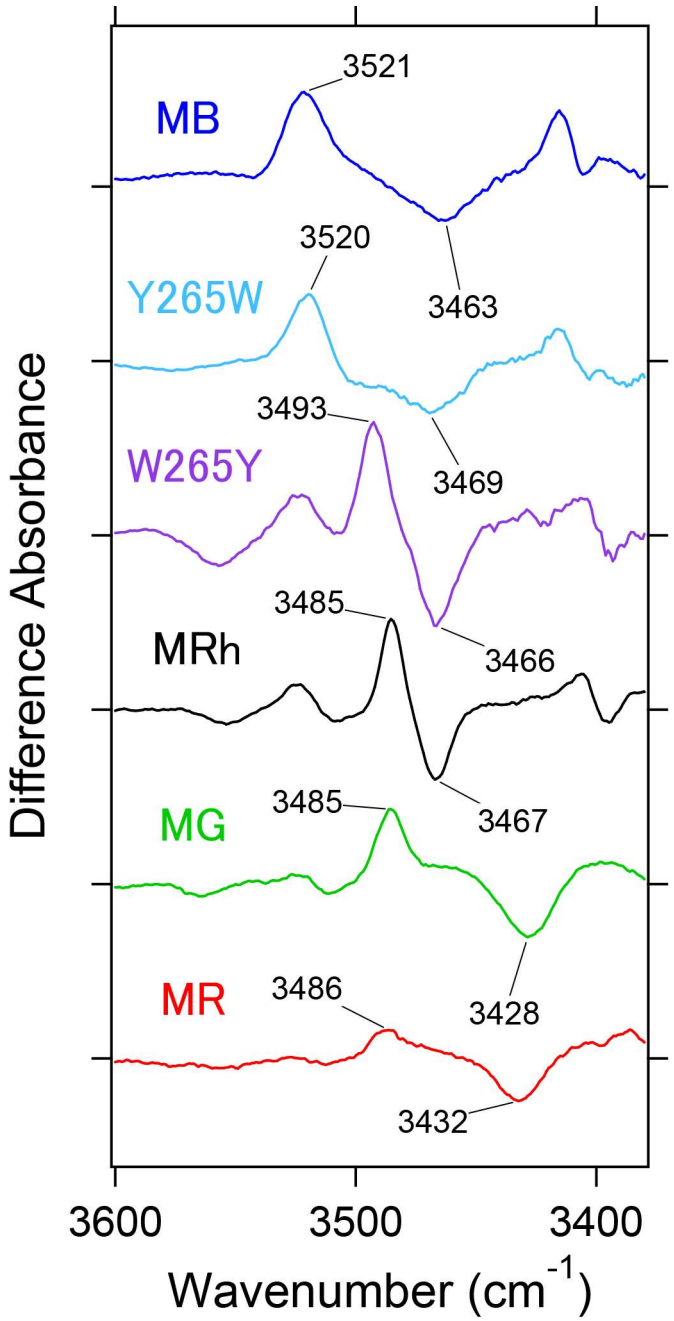
MB
3521
Y265W
3520
3463
W265Y
3493
3469
MRh
3485
3466
MG
3485
3467
MR
3486
3428
3432
Difference Absorbance
3600
3500
3400
Wavenumber (cm-1)

Figure S8

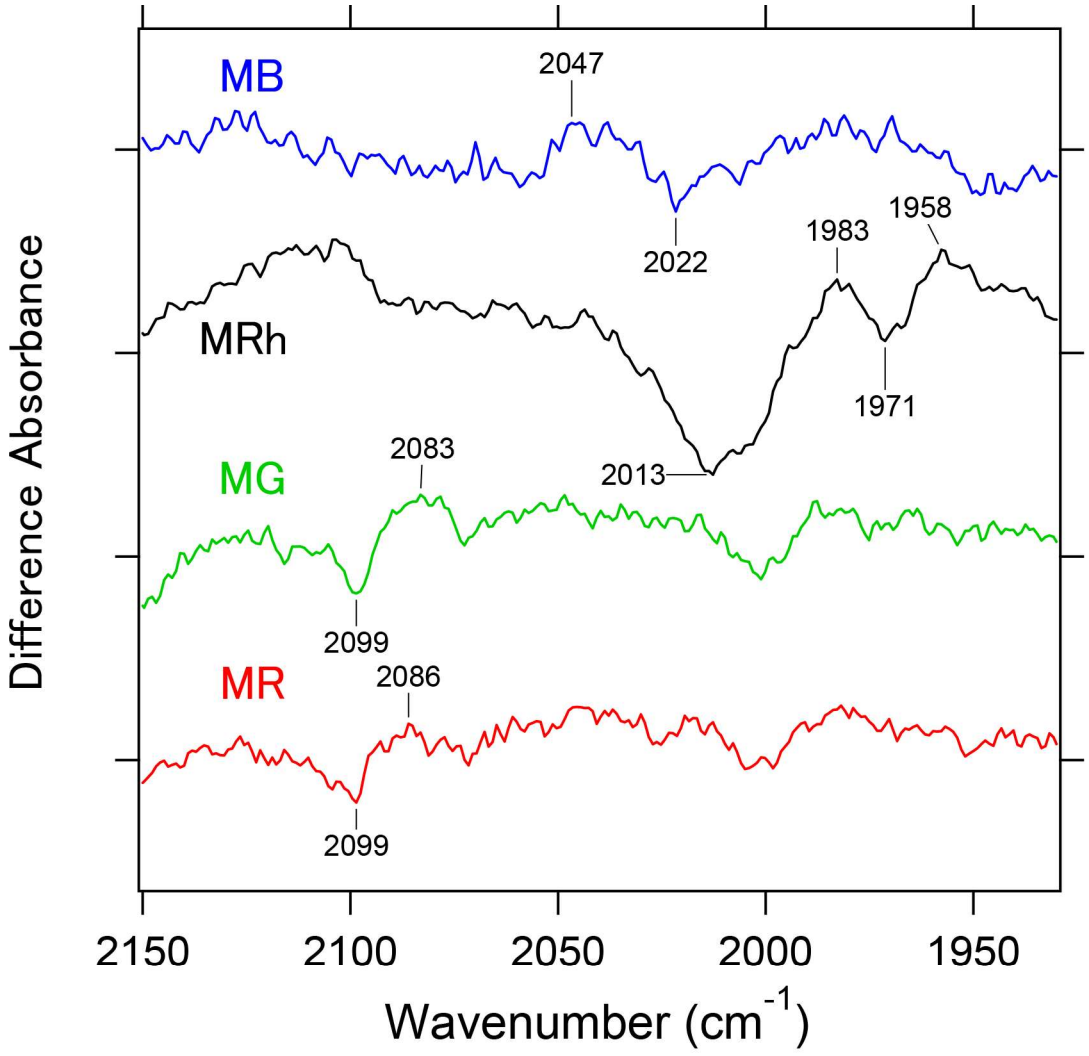
MB
2047
2022
MRh
1983
1958
1971
2013
MG
2083
2099
MR
2086
2099
Difference Absorbance
2150
2100
2050
2000
1950
Wavenumber (cm-1)